Potent *s-cis*-Locked Bithiazole Correctors of ΔF508 Cystic Fibrosis Transmembrane Conductance Regulator Cellular Processing for Cystic Fibrosis Therapy[⊥]

Gui Jun Yu,[†] Choong L. Yoo,[†] Baoxue Yang,[‡] Michael W. Lodewyk,[†] Liping Meng,[†] Tamer T. El-Idreesy,[†] James C. Fettinger,[†] Dean J. Tantillo,[†] A. S. Verkman,[‡] and Mark J. Kurth*[,†]

Department of Chemistry, University of California—Davis, One Shields Avenue, Davis, California 95616, and Department of Medicine and Physiology, University of California—San Francisco, San Francisco, California 94143-0521

Received May 8, 2008

N-(5-(2-(5-Chloro-2-methoxyphenylamino)thiazol-4-yl)-4-methylthiazol-2-yl)pivalamide **1** (compound **15Jf**) was found previously to correct defective cellular processing of the cystic fibrosis protein ΔF508-CFTR. Eight C4′−C5 C,C-bond-controlling bithiazole analogues of **1** were designed, synthesized, and evaluated to establish that constraining rotation about the bithiazole-tethering has a significant effect on corrector activity. For example, constraining the C4′-C5 bithiazole tether in the *s-cis* conformation [*N*-(2-(5-chloro-2-methoxyphenylamino)-7,8-dihydro-6*H*-cyclohepta[1,2-*d:*3,4-*d*′]bithiazole-2′-yl)pivalamide, **29**] results in improved corrector activity. Heteroatom placement in the bithaizole core is also critical as evidenced by the decisive loss of corrector activity with *s-cis* constrained *N*-(2-(5-chloro-2-methoxyphenylamino)-5,6-dihydro-4*H*-cycloheptа[1,2-*d:*3,4-*d*′]bithiazole-2′-yl)pivalamide **33**. In addition, computational models were utilized to examine the conformational preferences for select model systems. Following our analysis, the "*s-cis*-locked" cycloheptathiazolothiazole **29** was found to be the most potent bithiazole corrector, with an IC_{50} of ∼450 nM.

Introduction

Cystic fibrosis (CF[a]), an inherited disease that afflicts ∼1 in 2500 Caucasian individuals,[1] is caused by mutations in the CF transmembrane conductance regulator (CFTR) gene. The CFTR gene encodes a cAMP-regulated chloride channel expressed at the apical membrane of epithelial cells in various tissues (lung, pancreas, testes, and others[2,3]) with the primary cause of mortality being chronic lung infection and deterioration of lung function. ΔF508-CFTR, the most common CF-producing mutation, has a phenylalanine deletion at residue 508 of CFTR and is present in at least one allele of ∼90% of CF patients.[1] ΔF508-CFTR is misfolded, retained at the endoplasmic reticulum (ER), and rapidly degraded.[4] Despite the multiplicity of cellular defects associated with the ΔF508 mutation, small-molecule therapy of CF caused by the ΔF508 mutation is thought to have considerable promise.[5,6] Such therapy may require compounds with two complementary modes of action: a "corrector" to facilitate ΔF508-CFTR folding and plasma membrane targeting; a "potentiator" to improve ΔF508-CFTR chloride channel function. However, a highly effective corrector that restores normal folding of ΔF508-CFTR may obviate the need for a separate potentiator. Nanomolar-potency ΔF508-CFTR potentiators have already been identified and characterized.[6]

The complex, multistep nature of protein folding and trafficking presents a significant challenge in identifying potent, selective correctors of defective ΔF508-CFTR cellular processing. We previously reported the identification and characterization of ΔF508-CFTR correctors by screening a collection of 150,000 diverse small molecules utilizing Fischer rat thyroid (FRT) epithelial cells coexpressing ΔF508-CFTR and the halide-sensitive fluorescent protein YFP-H148Q/I152L.[7] ΔF508-CFTR-facilitated iodide influx was determined for each test compound by the kinetics of decreasing YFP fluorescence following addition of extracellular iodide in the presence of the potentiators genistein[8] and forskolin.[6,9]

Chart 1. Small Molecule Bithiazole Correctors of ΔF508-CFTR[11]

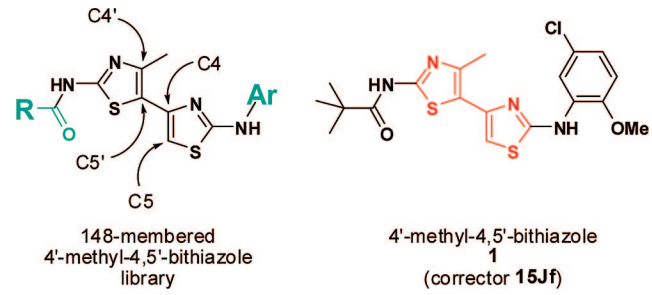

Analyses of the specificity, cellular mechanism, and efficacy in human CF cells of four chemical classes of active compounds identified from the screen established methylbithiazoles[10] as the most promising for further development. A subsequent synthesis and screening study of 148 methylbithiazole analogues focused on the peripheral amide and aniline substructures (e.g., blue substructures in the generalized methylbithiazole depicted in Chart 1) established initial structure activity relationship (SAR) data for this class of correctors with methylbithiazole corrector **1** (compound **15Jf** in our previous study) having the greatest corrector efficacy.[11] The purpose of the study here was to explore the bithiazole core structure of **1** (red substructure in **1**,

[⊥] X-ray crystallographic data of *N*-(2-(5-chloro-2-methoxyphenylamino)-7,8-dihydro-6*H*-cyclohepta[1,2-*d*:3,4-*d*′]bithiazole-2′-yl)pivalamide (**29**, $C_{21}H_{23}ClN_4O_2S_2$) were submitted to the Cambridge Crystallographic Data Centre (deposition number CCDC687310).

* To whom correspondence should be addressed. Telephone: (530) 752-8192. Fax: (530) 752-8995. E-mail: mjkurth@ucdavis.edu.

[†] University of California—Davis.

[‡] University of California—San Francisco.

[a] Abbreviations: CFTR, cystic fibrosis transmembrance conductance regulator; SAR, structure−activity relationship; CF, cystic fibrosis; ER, endoplasmic reticulum; FRT, Fischer rat thyroid; cAMP, cyclic adenosine monophosphate; YFP, yellow fluorescent protein.

10.1021/jm800533c CCC: $40.75
Published on Web 09/13/2008

Scheme 1. Synthesis of **7**[a]

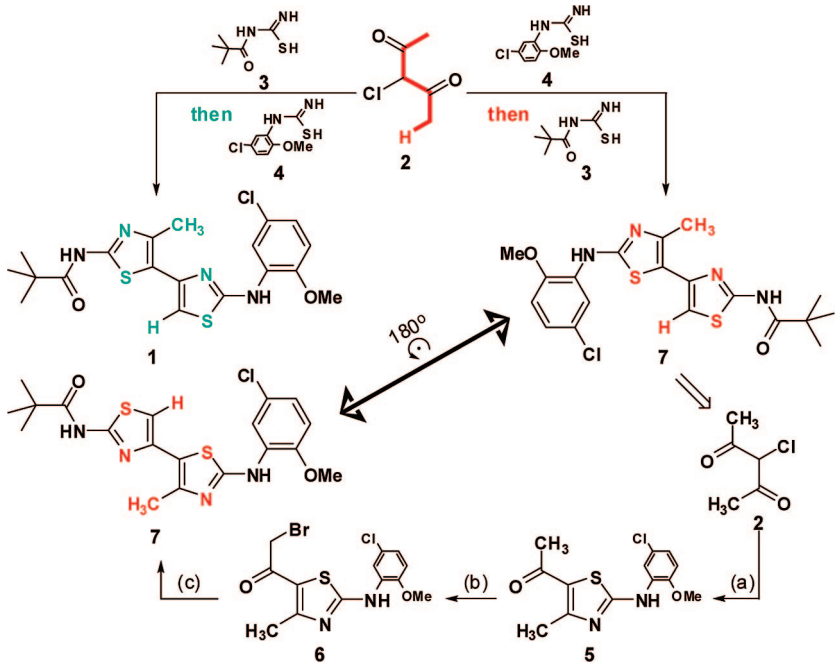

[a] Reagents: (a) **4**, EtOH, reflux; (b) pyridinium tribromide, 33% wt HBr in HOAc, room temperature; (c) (i) thiourea, EtOH, reflux; (ii) pivaloyl chloride, TEA, CH_3CN, THF, reflux.

Chart 1) to establish requisite structural features of the bis-heterocyclic portion of bithiazole ΔF508-CFTR correctors.

Results and Discussion

The first objective was to determine if the bithiazole substructure of **1** plays a crucial role in ΔF508-CFTR corrector activity or if it simply orchestrates the proper three-dimensional placement of the flanking pivalamide and 5-chloro-2-methoxyaniline substructures. To accomplish this, the two-fold symmetry of 3-chloropentane-2,4-dione (**2**)[12] was divergently exploited to prepare, from this one starting material, both **1**[11] and **7** as detailed in Scheme 1. The preparation of corrector **1** was accomplished by condensation of chlorodiketone **2** with *N*-pivaloylcarbamimidothioic acid (**3**)[13] to give a 1-(thiazol-5-yl)ethanone intermediate.[11] Bromination[14] α to the carbonyl of this thiazole and subsequent condensation with *N*-(5-chloro-2-methoxyphenyl)carbamimidothioic acid (**4**) delivers **1**. By transposition of the thiazole formation order, analogue **7** is obtained from the same starting material (**2**) as **1**. That is, condensation of **2** first with **4** followed by α-bromination and subsequent condensation with the equivalent of **3** (e.g., thiourea condensation followed by *N*-acylation with pivaloyl chloride) delivers transposed bithiazole **7** where the bithiazole core has been inverted relative to the topography set by the appended pivalamide and 5-chloro-2-methoxyaniline substructures (compare blue substructures in **1** with red substructures in bithiazole transposed **7** in Scheme 1).

Figure 1 shows that this bithiazole transposition in **7** results in near complete loss of ΔF508-CFTR corrector activity as assayed in FRT epithelial cells stably coexpressing human ΔF508-CFTR and the high-sensitivity halide-sensing fluorescent protein YFP-H148Q/I152L as described previously.[6] Since the conformational biases of **1** and **7** should be nearly identical, this dramatic change in corrector activity has three important implications: (i) proper three-dimensional display of the pivalamide and 5-chloro-2-methoxyaniline substructures is insufficient for corrector activity; (ii) the substituted bithiazole core

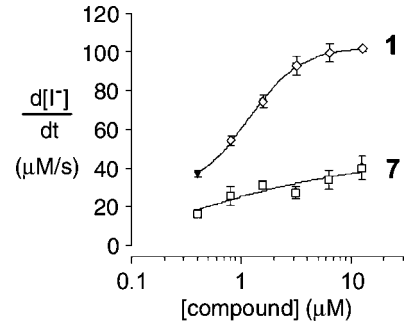

Figure 1. Activity−concentration profiles of **1** and **7**.

is a significant contributor to the activity of **1**; and (iii) while the target of **1** remains unknown, the remarkable activity differences for these two quite similar bithiazoles suggest that the activity of **1** may be the consequence of a specific ΔF508-CFTR binding event.

To initially explore the implications of (ii) above, the next objective was to partially modify the bithiazole core structure by replacing one of the thiazole rings with a phenyl ring. The chemistry to accomplish this objective is detailed in Scheme 2 and starts with 1-(3-aminophenyl)ethanone. *N*-Acylation of the aniline moiety with pivaloyl chloride was followed by bromination α to the carbonyl. Subsequent condensation of this bromoacetophenone with **4** delivered the 4-phenylthiazole analogue **10**. Starting with 1-(3-nitrophenyl)propan-1-one, a sequence consisting of bromination, thiazole formation, Sn(II)-mediated nitro reduction,[15] and subsequent *N*-acylation delivers the 5-methylthiazole analogue **13**. ΔF508-CFTR assay results for **10** and **13** reveal that each of these 4-phenylthiazole compounds has no ΔF508-CFTR corrector activity (see Figure S1 in Supporting Information).

The lack of corrector activity for **7**, **10**, and **13** is consistent with the bithiazole core being an important determinant of the corrector activity of **1**. We therefore designed bithiazole analogues that would probe structural and conformational

Scheme 2. Synthesis of 4-Phenylthiazole Analogues **10** and **13**[a]

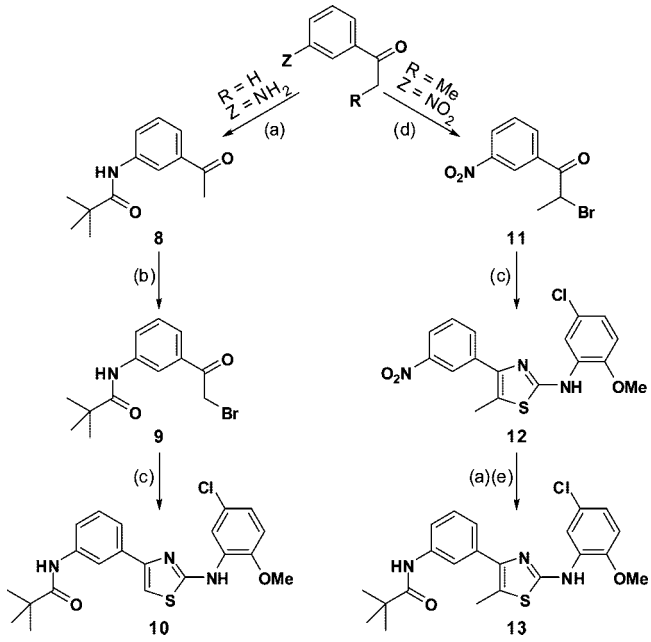

[a] Reagents: (a) pivaloyl chloride, TEA, $CHCl_3$, 0 °C; (b) pyridinium tribromide, 33% wt HBr in HOAc, room temperature; (c) **4**, EtOH, reflux; (d) Br_2, HOAc; (e) $SnCl_2 \cdot 2\ H_2O$, MeOH.

features of this central bis-heterocycle. One aspect of the 4′-methyl-4,5′-bithiazole moiety that could greatly affect its activity involves the dihedral angle of the thiazole-tethering C(4)−C(5′) bond (see Chart 1 for the numbering scheme). As depicted in Figure 2a, the 4′-methyl-4,5′-bithiazole system can adopt two approximately planar conformations: a conformation where the C(4′)−CH_3 substituent is *s-trans* to the C(5)−H and a conformation where the C(4′)−CH_3 substituent is *s-cis* to the C(5)−H. Interestingly, on the basis of quantum chemical calculations (Figure 2a), the *s-cis* conformer is actually slightly lower in energy (by ∼1 kcal/mol), despite the potential steric clash between the C(4′)−CH_3 and the C(5)−H. This appears to be the result of an attractive S···N interaction. Although there are precedents for S···X interactions,[16] we did not initially appreciate their relevance to our bithiazole systems. The relevance of such interactions to the conformations of thiazole-heterocycle systems was brought to our attention by Dr. Michael Bartberger (Amgen, personal communication to D.J.T. in 2007). Note that the preferred conformation of the amide group in **1** (that shown in Figure 2a) also displays an S···X interaction, in this case between a thiazole S and the amide carbonyl O.[17] The *s-trans* conformer is also twisted from planarity, although planarization of this structure (Figure 2a, left) is associated with a very small energetic penalty.[18] The barrier for conversion of the *s-cis* to the *s-trans* conformation is only 2−3 kcal/mol, so these structures are expected to interconvert freely in solution. However, as depicted in Figure 2b, the structural profiles of the *s-trans* and *s-cis* bithiazole conformations are quite distinct from one another in how they present bithiazole structural features such as H-bond donors, H-bond acceptors, and the hydrophobic C(4′)−CH_3. Two questions arise: does *s-trans*/*s-cis* conformational interplay influence the activity of **1**, and if so, would providing a conformational bias to this feature lead to improved activity?

It was initially reasoned that increasing the steric bulk of the C(5)-substituent on the bithiazole core would effectively preclude access to the *s-cis* conformation. The C(4′),C(5) dimethyl analogue **18** (see Scheme 3a) would have been our preferred target for this study because the presumed hydrophobic methyl pocket requirements of **1** would have been unperturbed. That target preference was, however, offset by retrosynthetic considerations. Just as symmetrical **2** is an ideal precursor to **1** because the first thiazole-forming condensation can occur redundantly on either carbonyl, 4-chloroheptane-3,5-dione is an ideal precursor to **17**, the C(4′)−CH_2CH_3/C(5)−CH_3 analogue of **1**. A similar retrosynthetic analysis of the C(4′)−CH_3/C(5)−CH_3 analogue of **18** points to unsymmetrical 3-chlorohexane-2,4-dione as the starting material, but **18** encounters a vexing carbonyl selectivity issue in the first thiazole-forming condensation reaction. For this reason, bithiazole **17** was selected as an initial probe of the *s-trans*/*s-cis* conformation questions. Its synthesis (with the pivalamide and 5-chloro-2-methoxyaniline substructures fixed as in **1**) was accomplished in four steps as outlined in Scheme 3a. Corrector activity assay revealed that **17**, while not as active as **1**, is a better corrector than **7**, **10**, and **13**, which supports the notion that the substituted bithiazole core is a critical contributor to the corrector activity of **1** (see Scheme 3b). A conformational profile for **17** is shown in Figure 3. Note that, despite the potential steric clash that was engineered into **17**, the *s-cis* conformer is again slightly lower in energy than the *s-trans* conformer. The *s-cis* minimum is now significantly distorted from planarity (twisted by ∼55°), however, presumably representing a compromise between the favorable S···N interaction and steric repulsion between the ethyl and methyl groups. The *s-trans* minimum is also more twisted than it was for **1**. Planarization of either of these structures is associated with a significant energetic penalty (Figure 3, far left and far right). Thus, if an approximately planar conformation, be it *s-trans* or *s-cis*, is required for binding, then the penalty associated with achieving such a conformation (3−7 kcal/mol) may account for the slightly reduced activity of **17** relative to **1**.

Since **17** is not as active as **1**, bithiazole analogue **22**, in which the C(4′)−CH_3 of **1** is replaced with a C(4′)−H to remove this impediment to achieving a planar conformation, was synthesized to determine if such an analogue would improve corrector activity. Retrosynthetic analysis of **22** (see Scheme 4) does not point back to a symmetric dicarbonyl starting material. Rather, the retrosynthetic precursor in this strategy would be 2-halo-3-oxobutanal, which is known as its bromo analogue. Indeed, 2-bromo-3-oxobutanal has been employed in the regioselective preparation of imidazole,[19] oxazole,[20] and thiazole[21] heterocycles. However, as an alternative option, a quite different route to 5-substituted-2-aminothiazoles starting from commercial 2-aminothiazole has been reported by Katritzky.[22] In that work, 2-aminothiazole is protected as its *N*,*N*-bis(trimethylsilyl) derivative and subsequently regioselective C(5)-lithiated. This latter route was selected for our work because this strategy could be readily used to introduce various groups at the C(5) position of the 2-aminothiazole ring. The C(4′),C(5)-unsubstituted analogue **22** was obtained in five steps from 2-aminothiazole as outlined in Scheme 4.

Figure 4a shows that **22** has an IC_{50} comparable to that of **1**. The *s-trans* and *s-cis* minima for bithiazole **22** are both planar and extremely close in energy (Figure 4b), providing circumstantial evidence that an approximately planar conformation of **22** is likely the active conformation.

Following from these insights with corrector **22**, we next investigated bithiazole methyl placement with analogue **25** (see Scheme 5). This compound is the C(4′)/C(5) methyl−hydrogen interchange analogue of **1**. By utilization of a modification of

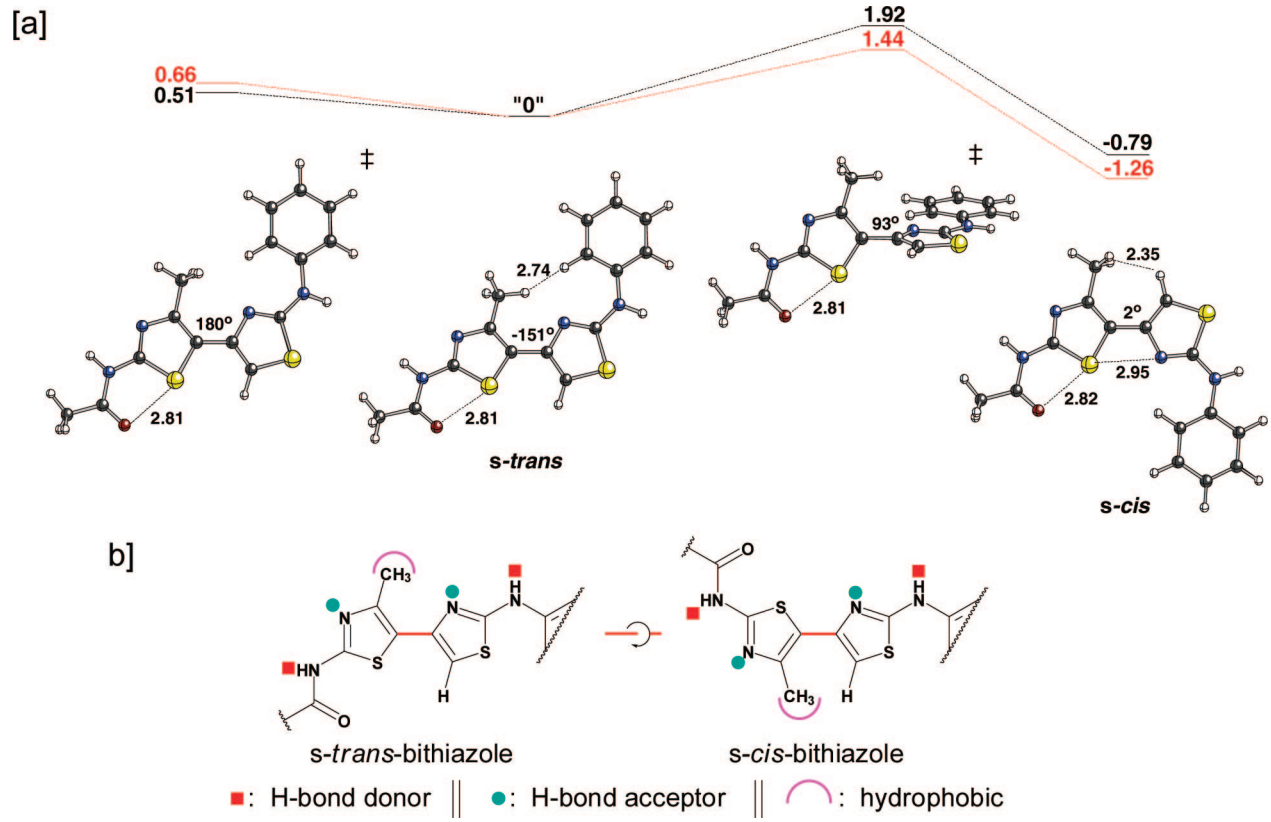

Figure 2. (a) Structures and associated energies for a model of **1**. From left to right, the structures shown are the transition state structure for interconversion of enantiomeric *s-trans* conformations, one enantiomeric *s-trans* minimum, the transition state structure for interconversion of the *s-trans* and *s-cis* minima, and the *s-cis* minimum. Associated energies are from B3LYP/6-31+G(d,p) (see Computational Methods for details). Selected distances are shown in Å; dihedral angles shown are for the central C−C−C−C substructure. Energies are in kcal/mol relative to the *s-trans* minimum. Gas-phase values are in black, and single point calculations in water are in red. (b) Structural consequences of a 180° rotation about the C(4)−C(5′) bithiazole bond.

Katritzky's 2-aminothiazole protection/C(5)-lithiation strategy employed in Scheme 4 but with replacement of acetaldehyde with propionaldehyde, the methyl−hydrogen transposed bithiazole **25** was obtained in five steps from 2-aminothiazole.

Figure 5 shows the corrector activity data of **25** compared with **1** and **22**. These data support the notion that methyl placement is important. Indeed, that **1** is a more effective corrector than **25** suggests that a C(4′)−CH_3 better addresses a hydrophobic binding pocket than does a C(5)−CH_3 placement.

The structure−activity relationships above support the notion that a planar bithiazole conformation is required for bithiazole ΔF508-CFTR corrector activity. While both **22** and **1** accommodate that requirement, neither constrains the bithiazole moiety to be planar nor do they predispose it in either the *s-cis* or *s-trans* conformation. To address these issues, the synthesis of conformationally locked analogues was undertaken, beginning with a compound constrained to be *s-cis*. Of the structural options considered, cycloheptathiazolothiazole **29** appeared to be the best *s-cis* alternative because (a) the corresponding cyclohexa analogue would be susceptible to aromatization (an event that would reduce solubility) and (b) precursors to the cycloocta analogue would be more difficult to prepare. Our route to **29** starts with cycloheptane-1,3-dione and is outlined in Scheme 6. Cycloheptathiazolothiazole **33**, the N ↔ S transposed isomer of **29**, was also prepared. The route to **33** is related to that used for the synthesis of **29** except that the 2-(5-chloro-2-methoxyanilino)thiazole heterocycle is now introduced first followed then by the 2-(*N*-pivalamido)thiazole heterocycle (Scheme 7) by analogy with the strategy outlined in Scheme 1.

The ΔF508-CFTR corrector activity data for cycloheptathiazolothiazoles **29** and **33** are shown relative to **22** and **1** in Figure 6a. Given that **29** is an effective corrector and cannot adopt an *s-trans* conformation, we conclude that an *s-cis* conformation is required for bithiazole activity. Moreover, the fact that bithiazole **17** is a relatively ineffective ΔF508-CFTR corrector supports the contention that an approximately planar *s-cis* conformation is ideal for maximizing activity. Our calculations indicate that the preferred conformation for **29** involves essentially coplanar thiazole rings (Figure 6b), although twisting from planarity by up to 25° is associated with a penalty of just over 1 kcal/mol (see Figure S2 in Supporting Information).

Correctors **29**, **22**, and **1** can readily adopt a conformation with coplanar thiazole rings, and consequently, each of these has strong ΔF508-CFTR corrector activity. The fact that *s-cis*-locked corrector **29** is the most active of these compounds is likely a result of removal of the entropy penalty expected upon binding by the conformationally flexible **1** and **22** by conformational preorganization in **29**.

Bithiazole **33**, the N ↔ S transposed isomer of **29**, is inactive even though it can place the pivalamide and 5-chloro-2-methoxyaniline substructures in similar orientations relative to the most active compound, corrector **29**. These data are consistent with proper placement of the four bithiazole heteroatoms being an important structural determinant in bithiazole ΔF508-CFTR corrector activity.

The final question regards the structure of the most potent activator cycloheptathiazolothiazole **29**; specifically, did the *N*-acylation with pivaloyl chloride occur at the 2-amino position

Scheme 3. Synthesis and Activity of **17**[a]

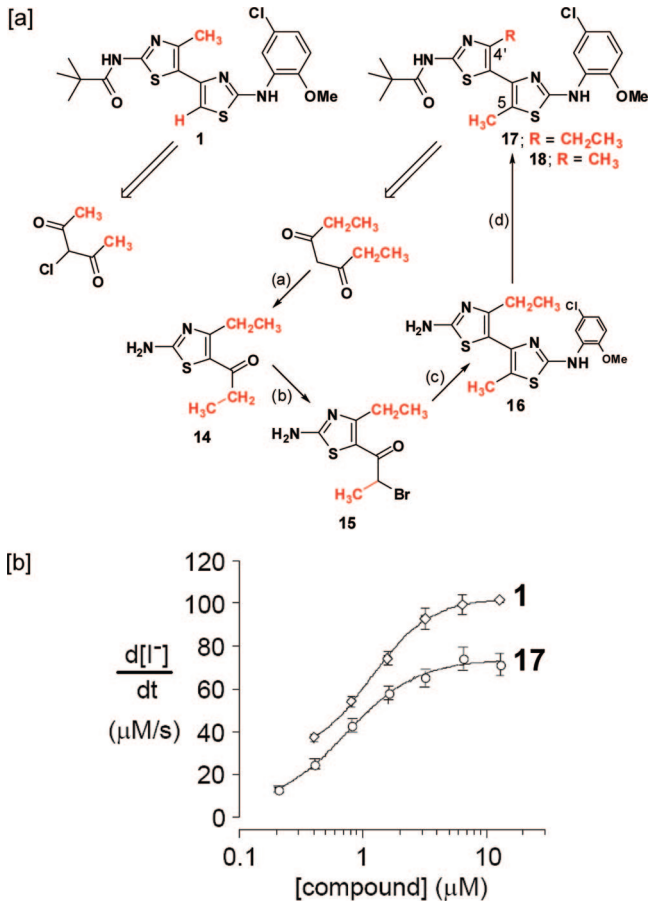

[a] [a] Reagents: (a) (i) Br_2, EtOH; (ii) thiourea, EtOH, room temperature; (b) Br_2, HOAc; (c) **4**, EtOH, reflux; (d) pivaloyl chloride, DCM, TEA, room temperature. [b] Activity−concentration analysis of **1** and **17** (mean ± SE, $n = 4$).

to give **29** or did this *N*-acylation occur to give one of the potential products **34**−**36** (see Chart 2)? Spectroscopic analysis of this reaction product proved difficult to unambiguously establish which product had been formed. Therefore, X-ray quality crystals were obtained and crystallographic analysis established that the sole product of this reaction was, indeed, **29**.

Conclusions

In conclusion, a systematic analysis of lead bithiazole core ΔF508-CFTR corrector **1** has been reported. Loss of corrector activity with analogues **7**, **10**, and **13** is consistent with the bithiazole substructure playing a central role in the activity of **1**. Conformational analysis of the thiazole-tethering C(4)−C(5′) bond suggested that two distinctly different conformations, one where the C(4′)−CH_3 substituent is *s-trans* to the C(5)−H and another where the C(4′)−CH_3 substituent is *s-cis* to the C(5)−H, are available to the 4′-methyl-4,5′-bithiazole moiety of **1**. Activity data for bithiazole analogues **17**, **22**, and **25** and the *s-cis*-locked analogue **29** and its transposed counterpart **33** indicate that an approximately planar *s-cis* bithiazole conformation, with proper placement of the four bithiazole heteroatoms, is likely the active presentation of **1**.

Experimental Section

Δ508-CFTR Corrector Activity Assay. FRT epithelial cells stably coexpressing human ΔF508-CFTR and the high-sensitivity halide-sensing fluorescent protein YFP-H148Q/I152L[7a] were used as described previously.[7b] Cells were grown at 37 °C (95% air/5% CO_2) for 24 h and then incubated for 16−20 h with 50 μL of medium containing the test compound. At the time of the assay, cells were washed with PBS and then incubated with PBS containing forskolin (20 μM) and genistein (50 μM) for 20 min. Measurements were carried out using FLUOstar fluorescence plate readers (Optima, BMG LABTECH Gmbh), each equipped with 500 ± 10 nm excitation and 535 ± 15 nm emission filters (Chroma Technology Corp.). Each well was assayed individually for I^- influx by recording fluorescence continuously (200 ms per point) for 2 s (baseline) and then for 12 s after rapid (<1 s) addition of 165 μL of PBS in which 137 mM Cl^- was replaced by I^-. I^- influx rate was computed by fitting the final 11.5 s of the data to an exponential for extrapolation of initial slope and normalizing for background-subtracted initial fluorescence. All experiments contained negative control (DMSO vehicle) and positive control [*N*-(2-(5-chloro-2-methoxyphenylamino)-4′-methyl-4,5′-bithiazol-2′-yl)benzamide].

1-{2-[(5-Chloro-2-methoxyphenyl)amino]-4-methyl-1,3-thiazol-5-yl}ethanone 5. A mixture containing **2** (0.67 g, 5 mmol) and **4** (1.08 g, 5 mmol) in absolute ethanol (25 mL) was refluxed for 24 h. When the reaction mixture was cooled in an ice bath, the product precipitated and was collected by filtration and washed with cold ethanol to afford **5** as a yellow-brown solid (0.82 g, 55%). ^{1}H NMR (600 MHz, DMSO-d_6): δ 10.17 (s, 1H), 8.41 (br s, 1H), 7.00−7.03 (m, 2H), 3.82 (s, 3H), 2.50 (s, 3H), 2.37 (s, 3H). ^{13}C NMR (150 MHz, DMSO-d_6): δ 189.5, 165.1, 155.9, 147.4, 130.2, 124.1, 123.3, 122.4, 118.9, 112.4, 56.1, 29.8, 18.5. MS *m*/*z* (ESI) 296.99 $(M + H)^+$.

2-Bromo-1-{2-[(5-chloro-2-methoxyphenyl)amino]-4-methyl-1,3-thiazol-5-yl}ethanone 6. To a solution of **5** (0.15 g, 0.5 mmol) in HBr/HOAc (33 wt % HBr in HOAc, 2.5 mL) was added pyridinium tribromide (0.18 g, 0.55 mmol). The reaction mixture was stirred at room temperature for 24 h and poured onto ice−water. The precipitated product was collected by filtration, washed with cold water, and dried to afford **6** (0.19 g, 99%). $R_f = 0.714$ in hexane/EtOAc, 1:1. ^{1}H NMR (600 MHz, DMSO-d_6): δ 8.38 (d, $J = 2.4$ Hz, 1H), 7.07−7.12 (m, 2H), 4.58 (s, 2H), 3.86 (s, 3H), 2.57 (s, 3H). ^{13}C NMR (150 MHz, DMSO-d_6): δ 183.1, 166.1, 158.1, 147.8, 129.8, 124.1, 123.1, 119.6, 119.4, 112.7, 56.2, 36.0, 18.7. MS *m*/*z* (ESI) 376.92 $(M + H)^+$.

***N*-(4-(2-(5-Chloro-2-methoxyphenylamineo)-4-methylthiazole-5-yl)thiazole-2-yl)pivalamide 7.** An absolute ethanol (8 mL) solution of **6** (0.19 g, 0.5 mmol) and thiourea (0.04 g, 0.5 mmol) was refluxed for 24 h. Upon completion of reaction, the solvent was removed by evaporation under reduced pressure and the residue was washed with chloroform and dried to give a pale-gray solid (0.15 g, 85%) which was used in the next step without purification.

Pivaloyl chloride (0.10 g, 0.85 mmol) was added dropwise to a CH_3CN/THF (1:1 v/v, 20 mL) solution of the crude material from above [*N*$^{2'}$-(5-chloro-2-methoxyphenyl)-4′-methyl-4,5′-bithiazole-2,2′-diamine; 0.15 g, 0.43 mmol] and triethylamine (0.09 g, 0.86 mmol) at room temperature. To effect starting material dissolution, the reaction mixture was warmed to reflux for 20 h. The reaction mixture was concentrated under vacuum, and the resulting residue was washed with chloroform and filtered. The filtrate was washed with water and dried (Na_2SO_4). Filtration followed by solvent removal under vacuum produced a residue that was subjected to preparative HPLC purification (UV detector, 224 nm; eluents H_2O (A), CH_3CN (B); gradients 0−1 min, 90% A; 1−13 min, 90−40% A; 13−18 min, 40−0% A; 18−21 min, 0% A; 21−21.5 min, 0−90% A; 21.5−25 min, 90% A). The product **7** was obtained as white needles (0.06 g, 34%). ^{1}H NMR (300 MHz, $CDCl_3$): δ 9.00 (s, 1H), 7.41 (d, $J = 2.1$ Hz, 1H), 7.23−7.27 (m, 2H), 6.93 (s, 1H), 6.90 (s, 1H), 3.89 (s, 3H), 2.55 (s, 3H), 1.34 (s, 9H). ^{13}C NMR (75 MHz, $CDCl_3$): δ 176.6, 167.5, 158.4, 151.7, 139.4, 134.4, 128.5, 127.8, 125.8, 123.6, 113.8, 113.3, 109.7, 56.5, 39.5, 27.4, 14.0. HRMS *m*/*z* (ESI) calcd for $C_{19}H_{21}ClN_4O_2S_2$ $(M + H)^+$ 437.0867, found 437.0867.

***N*-(3-Acetylphenyl)pivalamide 8.** To a stirred solution of 3-aminoacetophenone (1.0 g, 7.4 mmol) in chloroform cooled to 0 °C

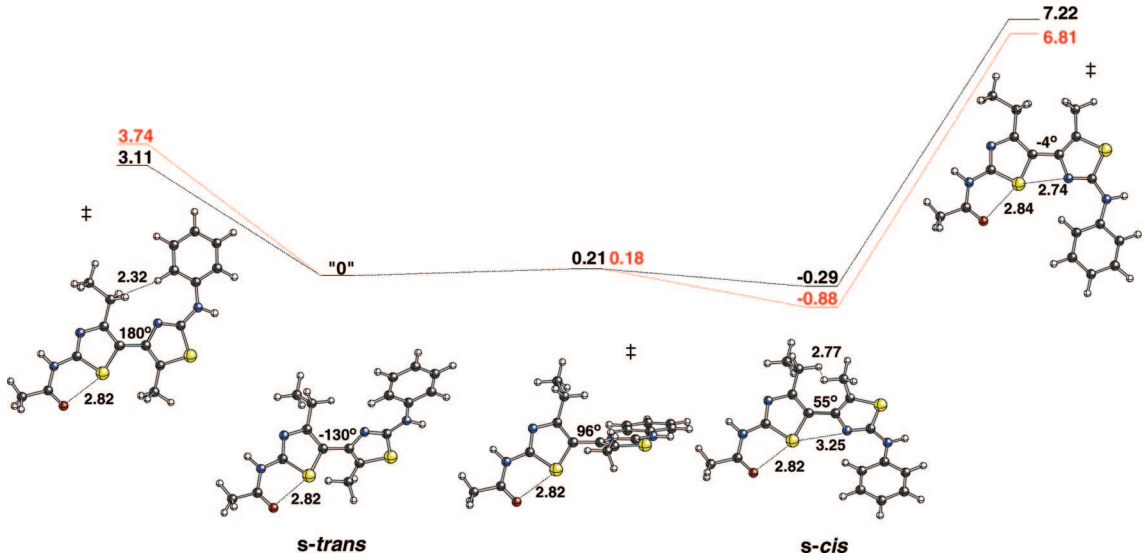

Figure 3. Structures and associated energies for a model of **17**. From left to right, the structures shown are the transition state structure for interconversion of enantiomeric *s-trans* conformations, one enantiomeric *s-trans* minimum, the transition state structure for interconversion of the *s-trans* and *s-cis* minima, one enantiomeric *s-cis* minimum, and the transition state structure for interconversion of enantiomeric *s-cis* conformations. The associated energies are from B3LYP/6-31+G(d,p) (see Computational Methods for details). Selected distances are shown in Å; dihedral angles shown are for the central C−C−C−C substructure. Energies are in kcal/mol relative to the s-*trans* minimum. Gas-phase values are in black, and single point calculations in water are in red.

Scheme 4. Synthesis of C(4′),C(5)-Unsubstituted Analogue **22**[a]

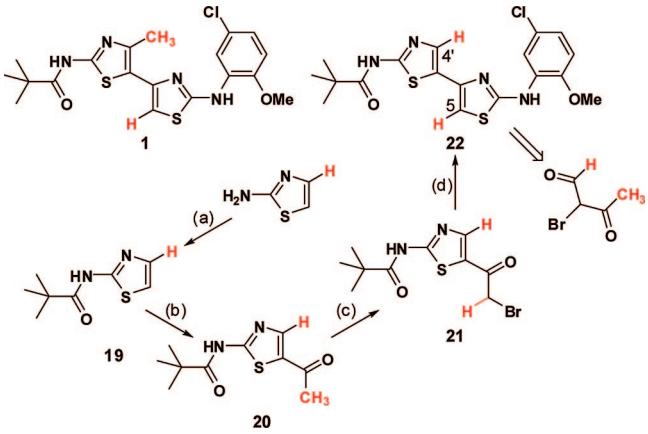

[a] Reagents: (a) pivaloyl chloride, DCM, TEA, room temperature; (b) (i) LDA, THF, then acetaldehyde; (ii) MnO_2, $CHCl_3$; (c) pyridinium tribromide, 33% wt HBr in HOAc, room temperature; (d) **4**, EtOH, reflux.

was added triethylamine dropwise (1.44 g, 14.2 mmol). The mixture was stirred for 15 min at this temperature. Then pivaloyl chloride (0.83 g, 7.4 mmol) was added dropwise, and the mixture was stirred overnight. Water was added, and the aqueous layer was extracted with DCM. The collected organic extracts were washed with saturated aqueous $NaHCO_3$ and brine, dried over anhydrous $MgSO_4$, and filtered. The solvent was evaporated under reduced pressure to afford **8** as a white solid (1.29 g, 80%). Mp 130−133 °C. ^{1}H NMR (600 MHz, $CDCl_3$): δ 8.07 (t, J = 1.8 Hz, 1H), 7.90−7.88 (m, 1H), 7.76 (br s, 1H), 7.65−7.63 (m, 1H), 7.37 (t, J = 1.8 Hz 1H), 2.57 (s, 3H), 1.31(s, 9H). ^{13}C NMR (150 MHz, $CDCl_3$): δ 198.2, 177.2, 138.8, 137.7, 129.3, 124.9, 124.1, 119.7, 39.8, 27.6, 26.8.

***N*-(3-(2-Bromoacetyl)phenyl)pivalamide 9.** To a stirred solution of *N*-(3-acetylphenyl)pivalamide **8** (0.30 g, 1.37 mmol) in 33% HBr in HOAc (5 mL) was added pyridinium tribromide (0.48 g, 1.51 mmol). The mixture was stirred at room temperature for 24 h and then poured into ice-cold water. The organic layer was extracted with DCM, washed with saturated aqueous $NaHCO_3$ and brine, dried over anhydrous $MgSO_4$, and filtered. Evaporation of the solvent afforded **9** (0.32 g, 78%) which was used in the next step without further purification. ^{1}H NMR (600 MHz, $CDCl_3$): δ 8.08 (t, J = 1.8 Hz, 1H), 7.94 (br s, 1H), 7.82 (dt, J = 8.4, 1.2 Hz, 1H), 7.60 (dd, J = 7.2 Hz, 1.2 Hz, 1H), 7.32 (t, J = 7.8 Hz, 1H), 4.30 (s, 2H), 1.27 (s, 9H). ^{13}C NMR (150 MHz, $CDCl_3$): δ 191.2, 177.3,

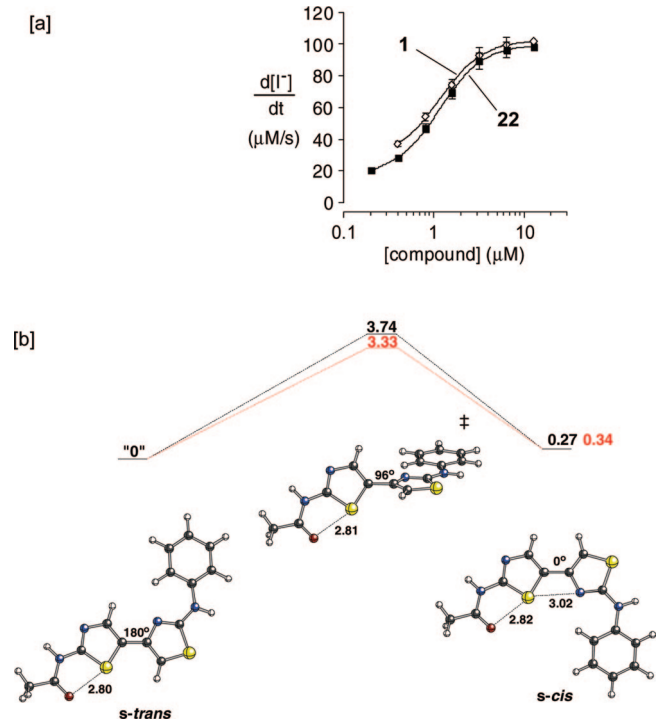

Figure 4. (a) Activity−concentration profiles of **1** and **22**: P = pivalamide and A = 5-chloro-2-methoxyaniline. (b) Structures and associated energies for a model of **22**. From left to right, the structures shown are the *s-trans* minimum, the transition state structure for interconversion of the *s-trans* and *s-cis* minima, and the *s-cis* minimum. The associated energies are from B3LYP/6-31+G(d,p) (see Computational Methods for details). Selected distances are shown in Å; dihedral angles shown are for the central C−C−C−C substructure. Energies are in kcal/mol relative to the s-*trans* minimum. Gas-phase values are in black, and single point calculations in water are in red.

Scheme 5. Synthesis of **25**[a]

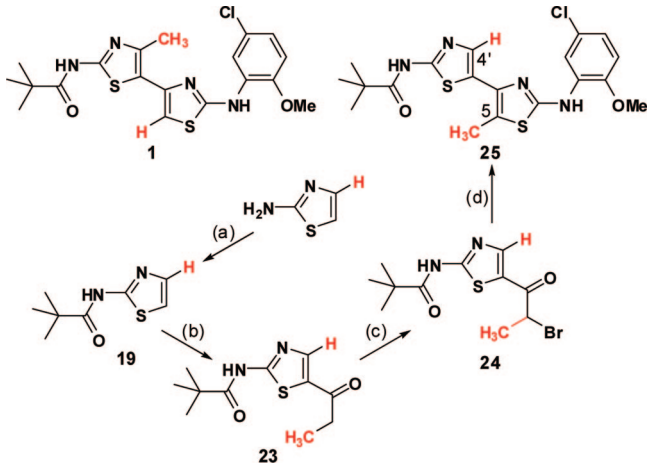

[a] Reagents: (a) pivaloyl chloride, DCM, TEA, room temperature; (b) (i) LDA, THF, then propionaldehyde; (ii) MnO_2, $CHCl_3$; (c) pyridinium tribromide, 33% wt HBr in HOAc; room temperature; (d) **4**, EtOH, reflux.

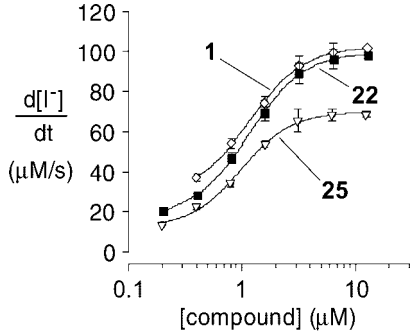

Figure 5. Activity−concentration profile of **25** compared to **1** and **22**.

Scheme 6. Synthesis of Cycloheptathiazolothiazole Analogue **29**[a]

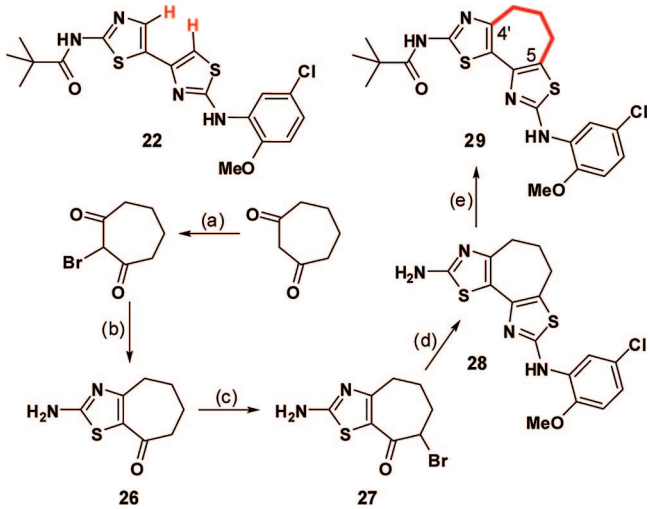

[a] Reagents: (a) Br_2, CCl_4/H_2O, room temperature; (b) thiourea, EtOH, room temperature; (c) Br_2 in HOAc, room temperature; (d) **4**, EtOH, reflux; (e) pivaloyl chloride, DCM, TEA, room temperature.

139.0, 134.4, 129.3, 125.8, 124.4, 120.4, 39.7, 31.4, 27.5. MS *m/z* (ESI) 298.06 $[M + H]^+$, 300.02 $[(M + 2) + H]^+$.

***N*-(3-(2-(5-Chloro-2-methoxyphenylamino)thiazol-4-yl)phenyl)pivalamide 10.** A mixture of **9** (0.32 g, 1.06 mmol) and **4** (0.23 g, 1.06 mmol) in ethanol was refluxed for 48 h. The solvent was

Scheme 7. Synthesis of Cycloheptathiazolothiazole Analogue **33**[a]

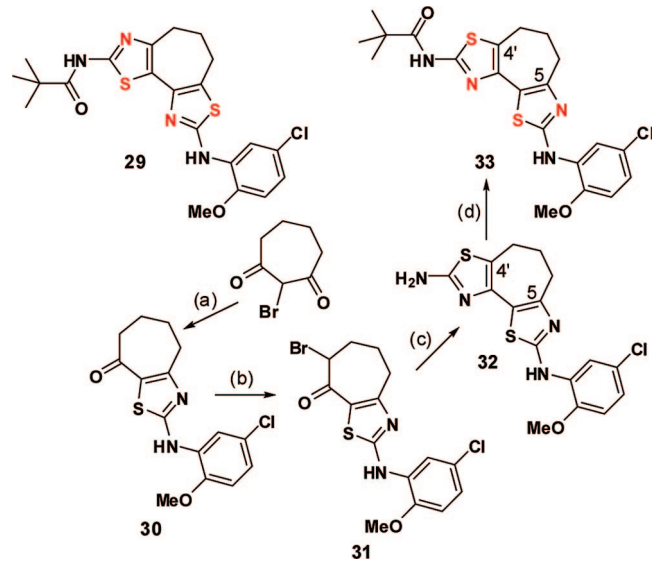

[a] Reagents: (a) **4**, EtOH, reflux; (b) Br_2 in HOAc, room temperature; (c) thiourea, EtOH, reflux; (d) pivaloyl chloride, DCM, TEA, room temperature.

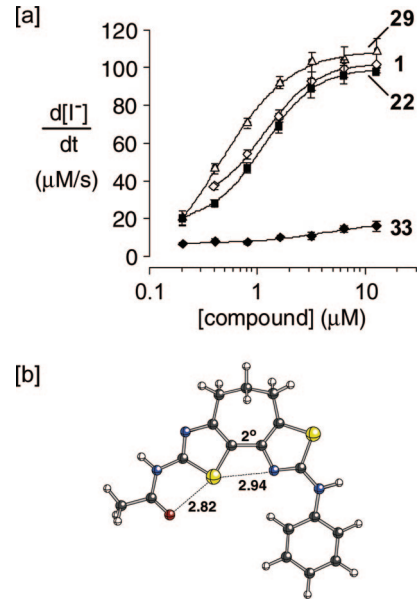

Figure 6. (a) Activity−concentration profile of corrector **29** relative to **1**, **22**, and **33**. (b) Structure of the conformational minimum for a model of **29**. The structure is from B3LYP/6-31+G(d,p) (see Computational Methods for details). Selected distances are shown in Å; dihedral angles shown are for the central C−C−C−C substructure.

evaporated, and the residue was purified by preparative HPLC to afford **10** as a white-gray solid (0.32 g, 73%). Mp 137−138 °C. ^{1}H NMR (300 MHz, $CDCl_3$): δ 7.99 (s, 1H), 7.82 (m, 1H), 7.67 (s, 1H), 7.48 (d, $J = 2.4$ Hz, 1H), 7.42 (m, 1H), 7.25 (m, 1H), 6.93 (d, $J = 8.7$ Hz, 1H), 6.73 (s, 1H), 3.89 (s, 3H), 1.34 (s, 9H). ^{13}C NMR (75 MHz, $CDCl_3$): δ 177.4, 169.6, 151.2, 142.8, 139.3, 129.2, 128.2 127.7, 126.0, 123.4, 2 × 121.3, 117.7, 113.2, 100.2, 56.3, 39.9, 27.6. HRMS *m/z* (ESI) calcd for $C_{21}H_{22}ClN_3O_2S$ $(M + H)^+$ 416.1194, found 416.1193.

2-Bromo-1-(3-nitrophenyl)propan-1-one 11. To a stirred solution of 1-(3-nitrophenyl)propan-1-one (1.41 g, 7.90 mmol) in acetic acid (20 mL) was added bromine dropwise (1.27 g, 7.93 mmol), and the mixture was stirred at room temperature for 24 h. The mixture was poured into ice-cold water, and the organic layer was extracted with DCM. The organic extract was washed with saturated aqueous

Chart 2. Chemoselective *N*-Acylation of the Cycloheptathiazolothiazole Heterocycle

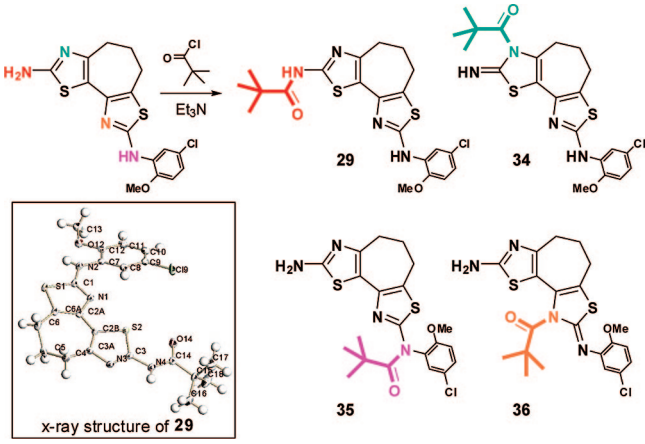

$NaHCO_3$ and brine, dried over anhydrous $MgSO_4$, and filtered. Evaporation of the solvent under reduced pressure afforded **11** as a white solid[23] which was used in the next step without further purification (1.78 g, 87%). ^{1}H NMR matches literature data.[23]

***N*-(5-Chloro-2-methoxyphenyl)-5-methyl-4-(3-nitrophenyl)thiazol-2-amine 12.** A mixture of **11** (0.50 g, 1.94 mmol) and **4** (0.42 g, 1.94 mmol) in ethanol was refluxed for 24 h. The mixture was cooled to room temperature and the precipitate was collected by filtration to afford **12** as a yellow solid (0.57 g, 78%). Mp decomposition at 185 °C. ^{1}H NMR (300 MHz, DMSO-d_6): δ 8.64 (m, 1H), 8.50 (m, 1H), 8.15 (m, 2H), 7.73 (m, 1H), 6.96 (m, 2H), 4.84 (br s, 1H), 3.87 (s, 3H), 2.48 (s, 3H). ^{13}C NMR (150 MHz, DMSO-d_6): δ 159.4, 148.0, 146.4, 141.9, 136.4, 131.2, 124.3, 120.5, 133.6 130.0, 122.1, 121.6, 120.4, 116.9, 111.8, 56.0, 11.9. MS *m*/*z* (ESI) 376.06 $[M + H]^+$.

***N*-(3-(2-(5-Chloro-2-methoxyphenylamino)-5-methylthiazol-4-yl)phenyl)pivalamide 13.** A mixture of **12** (0.25 g, 0.66 mmol) and $SnCl_2 \cdot 2H_2O$ (1.35 g, 6.0 mmol) in methanol was refluxed for 48 h. Evaporation of the solvent under reduced pressure afforded 4-(3-aminophenyl)-*N*-(5-chloro-2-methoxyphenyl)-5-methylthiazol-2-amine as a solid which was dissolved in chloroform and cooled in an ice bath to 0 °C. Triethylamine (93 μL, 0.66 mmol) was added, and the mixture was stirred for 15 min at the same temperature. Pivaloyl chloride (0.08 g, 0.66 mmol) was then added dropwise at 0 °C, and the mixture was stirred overnight at which point the mixture was poured into ice-cold water and the aqueous layer was extracted with DCM. The collected organic extract was washed with saturated aqueous $NaHCO_3$ and brine, dried over anhydrous $MgSO_4$, and filtered. Evaporation of the solvent under reduced pressure afforded **13** as a yellowish white solid (0.21 g, 75%). Mp decomposition at 195 °C. ^{1}H NMR (300 MHz, $CDCl_3$): δ 7.83 (s, 1H), 7.76 (s, 1H), 7.45 (m, 1H), 7.38 (d, J = 2.40 Hz, 1H), 7.33 (s, 1H), 7.27 (m, 1H), 6.93 (d, J = 9.0 Hz, 1H), 3.89 (s, 3H), 2.42 (s, 3H), 1.33 (s, 9H). ^{13}C NMR (150 MHz, $CDCl_3$): δ 177.4, 168.4, 151.5, 139.1, 129.9, 127.8, 125.9, 124.3, 123.6, 121.3, 120.3, 118.5, 114.5, 113.3, 111.4, 111.0, 56.4, 39.9, 27.7, 12.5. HRMS *m*/*z* (ESI) calcd for $C_{22}H_{24}ClN_3O_2S$ $(M + H)^+$ 430.1351, found 430.1345.

1-(2-Amino-4-ethylthiazol-5-yl)propan-1-one 14.[24] An absolute ethanol solution of bromine (453 μL, 8.82 mmol) was added dropwise at room temperature to an absolute ethanol solution of 3,5-heptanedione (1.13 g, 8.82 mmol), and thiourea (5.11g, 8.82 mmol). The resulting reaction mixture was refluxed overnight, at which point the ethanol was evaporated in vacuo and the residue was triturated with a small quantity of DCM. The DCM was evaporated to dryness under reduced pressure, and the residue was treated with cold acetone. The resulting brown solid was collected by filtration and rinsed with cold acetone to afford **14** as a white powder (1.3 g, 80%). Mp decomposition at 133 °C. ^{1}H NMR matches literature data.[23]

1-(2-Amino-4-ethylthiazol-5-yl)-2-bromopropan-1-one 15. Compound **14** (0.53 g, 1.99 mmol; HBr form) in acetic acid (2 mL) was treated dropwise with bromine (103 μL, 1.99 mmol), and the reaction mixture was stirred at room temperature for 3 h. The white precipitate was collected by filtration and washed with cold acetone to yield **15** as a white powder (0.59 g, 86%). Mp decomposition at 122 °C. ^{1}H NMR (600 MHz, DMSO-d_6): δ 4.99 (q, J = 6 Hz, 1H), 2.88 (q, J = 6 Hz, 2H), 1.69 (d, J = 6 Hz, 3H), 1.16 (t, J = 6 Hz, 3H). ^{13}C NMR (150 MHz, DMSO-d_6): δ 185.5, 170.7, 115.5 × 2, 47.6, 47.5, 24.0, 20.8, 13.5. MS *m*/*z* (ESI) 263.00 $[M + H]^+$, 264.96 $[(M + 2) + H]^+$.

4-(2-Amino-4-ethylthiazol-5-yl)-*N*-(5-chloro-2-methoxyphenyl)-5-methylthiazol-2-amine 16. Compound **15** (0.56 g, 1.64 mmol) was dissolved in absolute ethanol (15 mL), and **4** (0.36 g, 1.64 mmol) was added at room temperature. The resulting suspension was stirred at reflux for 2 h. After removal of ethanol in vacuo, the solid was collected by filtration and washed with cold ethanol to yield **16** as a yellow powder (0.75 g, 99%). Mp decomposition at 133 °C. ^{1}H NMR (600 MHz, $CDCl_3$): δ 8.96 (br s, 2H), 7.79 (d, J = 2.4 Hz, 1H), 7.01 (dd, J = 8.4 Hz, 2.4 Hz, 1H), 6.82 (d, J = 8.4 Hz, 1H), 3.87 (s, 3H), 2.66 (q, J = 7.6 Hz, 2H), 2.29 (s, 3H), 1.33 (t, J = 7.6 Hz, 3H). ^{13}C NMR (150 MHz, DMSO-d_6): δ 169.6, 162.5, 148.0, 140.2, 128.8, 126.1, 124.5, 123.2, 119.1, 112.1, 56.5, 21.2, 18.6, 13.1. MS *m*/*z* (ESI) 380.97 $[M + H]^+$.

***N*-(5-(2-(5-Chloro-2-methoxyphenylamino)-5-methylthiazol-4-yl)-4-ethylthiazol-2-yl)pivalamide 17.** To a suspension of **16** (0.50 g, 1.1 mmol) in DCM (55 mL) was added TEA (395 μL, 2.84 mmol). Pivaloyl chloride (174 μL, 1.42 mmol) was then added to the suspension in one portion, and the reaction mixture was stirred at room temperature for 10 min at which time TLC indicated reaction completion. The reaction mixture was washed with cold water and extracted with DCM (2×). The organic layer was dried over anhydrous sodium sulfate and filtered, and DCM was removed in vacuo. The resulting solid was purified by silica gel column chromatography (hexane/ethyl acetate = 4:1 eluent) to yield **17** as a light-orange powder (0.34 g, 66%). Mp decomposition at 192 °C. ^{1}H NMR (400 MHz, $CDCl_3$): δ 7.72 (d, J = 2.8 Hz, 1H), 7.13 (dd, J = 8.8 Hz, 2.8 Hz, 1H), 6.88 (d, J = 8.8 Hz, 1H), 3.90 (s, 3H), 2.79 (q, J = 7.6 Hz, 2H), 2.30 (s, 3H), 1.39 (s, 9H), 1.34 (t, J = 7.6 Hz, 3H). ^{13}C NMR (100 MHz, $CDCl_3$): δ 178.6, 164.6, 164.2, 163.8, 162.2, 149.1, 144.9, 128.9, 125.5, 120.5, 113.8, 112.3, 104.9, 56.3, 40.1, 26.7, 21.4, 13.5, 12.2. HRMS *m*/*z* (ESI) calcd for $C_{21}H_{25}ClN_4O_2S_2$ $(M + H)^+$ 465.1180, found 465.1181.

***N*-(5-Acetylthiazol-2-yl)pivalamide 20.** Freshly distilled diisopropylamine (5.98 mL, 42.70 mmol) was dissolved in dry THF (30 mL) and cooled to −78 °C under nitrogen. This solution was treated dropwise with 2.5 M *n*-BuLi in hexane (17.1 mL, 42.70 mmol) and stirred for 30 min. A solution of **19**[25] (3.58 g, 19.41 mmol) in anhydrous THF (20 mL) was then added dropwise to this LDA solution and stirred for 30 min at −78 °C, at which time acetaldehyde (3.59 mL, 64.05 mmol) was added dropwise. The resulting mixture was stirred overnight as it warmed to ambient temperature. The reaction was quenched by dropwise addition of water, diluted with DCM (3× the THF volume), washed with water, dried over anhydrous sodium sulfate, and filtered. After removal of solvents, the resulting crude material was used in the next step without purification.

This crude material (0.80 g, 3.50 mmol) was dissolved in $CHCl_3$ (35 mL), manganese dioxide (9 g, 104 mmol) was added, and the resulting mixture was stirred at room temperature overnight. Filtration of the reaction mixture through a pad of Celite and chloroform removal gave crude product which was purified by silica gel column chromatography (hexane/ethyl acetate = 4:1 eluent) to yield **20** as a white powder (0.42 g, 53%). ^{1}H NMR (300 MHz, $CDCl_3$): δ 10.0 (br s, 1H), 7.98 (s, 1H), 2.48 (s, 3H), 1.29 (s, 9H).

***N*-(5-(2-Bromoacetyl)thiazol-2-yl)pivalamide 21.** Compound **20** (0.26 g, 1.15 mmol) was dissolved in 33% HBr in HOAc (100 mL), pyridinium tribromide (0.37 g, 1.15 mmol) was added, and the mixture was stirred at room temperature overnight. The reaction mixture was poured onto ice−water and the solid was collected by filtration to yield **21** which was in the next step without purification (0.34 g, 97%). ^{1}H NMR (400 MHz, $CDCl_3$): δ 8.12 (s, 1H), 4.27 (s, 2H), 1.36 (s, 9H).

***N*-(2-(5-Chloro-2-methoxyphenylamino)-4,5′-bithiazol-2′-yl)pivalamide 22.** A suspension of **21** (0.73 g, 2.3 mmol) and *N*-(5-chloro-2-methoxyphenyl)thiourea (0.73 g, 2.53 mmol) in EtOH (25 mL) was refuxed for 30 min. When the mixture was cooled, the product was collected by filtration and washed with cold ethanol to yield **22** as a pale-yellow solid (0.40 g, 84%). Mp decomposition at 216 °C. ^{1}H NMR (600 MHz, DMSO-d_6): δ 11.86 (br s, 1H) 9.93 (br s, 1H), 8.64 (d, J = 2.4 Hz, 1H), 7.83 (s, 1H), 7.18 (s, 1H), 7.02 (d, J = 8.4 Hz, 1H), 6.98 (dd, J = 8.4 Hz, 2.4 Hz, 1H), 3.86 (s, 3H), 1.25 (s, 9H). ^{13}C NMR (150 MHz, DMSO-d_6): δ 176.7, 162.1, 158.9, 146.6, 140.2, 136.4, 130.5, 124.7, 124.2, 121.3, 117.3, 112.1, 91.0, 56.1, 38.8, 26.6. HRMS *m*/*z* (ESI) calcd for $C_{18}H_{19}ClN_4O_2S_2$ $(M + H)^+$ 423.0711, found 423.0713.

***N*-(5-Propionylthiazol-2-yl)pivalamide 23.** Following the protocol outlined for **20** gave **23** as an off-white powder (0.78 g, 52%). Mp decomposition at 126 °C. ^{1}H NMR (400 MHz, $CDCl_3$), δ 9.23 (br s, 1H), 8.03 (s,1H), 2.88 (q, J = 8 Hz, 2H), 1.34 (s, 9H), 1.23 (t, J = 8 Hz, 3H). MS (ESI) *m*/*z* 241.07 $[M + 1]^+$.

***N*-(5-(2-Bromopropanoyl)thiazol-2-yl)pivalamide 24.** Following the protocol outlined for **21** gave **24** (0.73 g, 71%) as an off-white powder. Mp decomposition at 192 °C. ^{1}H NMR (400 MHz, $CDCl_3$): δ 8.25 (s, 1H), 5.02 (q, J = 6.8 Hz, 1H), 1.87 (d, J = 6.8 Hz, 3H), 1.35 (s, 9H). MS *m*/*z* (ESI) 319.04 $[M + H]^+$, 321.00 $[(M + 2) + H]^+$.

***N*-(2-(5-Chloro-2-methoxyphenylamino)-5-methyl-4,5′-bithiazol-2′-yl)pivalamide 25.** Following the protocol outlined for **22** gave **25**. Mp decomposition at 221 °C. ^{1}H NMR (600 MHz, DMSO-d_6): δ 11.79 (br s, 1H), 9.73 (br s, 1H), 8.57 (d, J = 3 Hz, 1H), 7.67 (s, 1H), 7.01 (d, J = 8.4 Hz, 1H), 6.96 (dd, J = 8.4 Hz, 3 Hz, 1H), 3.86 (s, 3H), 2.43 (s, 3H), 1.26 (s, 9H). ^{13}C NMR (150 MHz, DMSO-d_6): δ 176.5, 159.6, 157.9, 146.5, 136.7, 134.0, 131.2, 126.4, 124.3, 120.6, 117.0, 116.9, 112.0, 56.1, 38.8, 26.6, 11.7. HRMS *m*/*z* (ESI) calcd for $C_{19}H_{21}ClN_4O_2S_2$ $(M + H)^+$ 437.0867, found 437.0868.

2-Amino-6,7-dihydro-4*H*-cyclohepta[*d*]thiazol-8(5*H*)-one 26. Following the procedure reported by Ragan[26a] afforded cycloheptane-1,3-dione as clear and colorless oil. IR cm^{-1}: 2949, 2870, 1716, 1696 (lit. 1716, 1693). Bp 70 °C at 0.3 mmHg. ^{1}H NMR matches literature data.[25]

To a 0 °C biphasic mixture of cycloheptane-1,3-dione (5.7 g, 45.17 mmol) in CCl_4/deionized water (1:1; 150 mL) was added (dropwise) Br_2 (2.55 mL, 49.7 mmol) in CCl_4 (75 mL). The mixture was stirred at 0 °C for 1 h and extracted with DCM, and the organic layer was collected. DCM was removed under reduced pressure at room temperature to afford 2-bromocycloheptane-1,3-dione which was used to the next step without further purification.

To a solution of 2-bromocycloheptane-1,3-dione (45.17 mmol) in absolute EtOH (100 mL) was added thiourea (3.61 g, 47.43 mmol). The reaction mixture was stirred at room temperature overnight at which point the EtOH was removed under reduced pressure and the resulting dark-orange residue was triturated with DCM. The residue was recrystallized from EtOH to afford **26** as an off-white solid (6 g, 50% overall crude yield from cycloheptane-1,3-dione). ^{1}H NMR (300 MHz, DMSO-d_6): δ 8.87 (br s, 2H), 2.87 (t, J = 6 Hz, 2H), 2.64 (t, J = 6 Hz, 2H), 1.89−1.85 (m, 2H), 1.81−1.77 (m, 2H).

2-Amino-7-bromo-6,7-dihydro-4*H*-cyclohepta[*d*]thiazol-8(5*H*)-one 27. Compound **26** (1.96 g, 7.45 mmol; HBr salt form) in glacial acetic acid (70 mL) was treated dropwise with Br_2 (421 μL, 8.2 mmol). The reaction mixture was stirred at room temperature for 30 min. The crude product was collected by filtration, washed with cold acetone, and dried to yield **27** which was used in the next step without purification (1.98 g, 78%). ^{1}H NMR (600 MHz, DMSO-d_6): δ 8.71 (br s, 2H), 5.11 (dd, J = 6.9 Hz, 3.3 Hz, 1H), 3.08−2.90 (m, 2H), 2.47−2.39 (m, 1H), 2.28−2.20 (m, 1H), 2.14 (dd, J = 10.1 Hz, 2.3 Hz, 1H), 1.98 −1.90 (m, 1H). MS (ESI) *m*/*z* $[M + H]^+$ 260.92; $[(M + 2) + H]^+$ 262.88.

***N*^{2}-(5-Chloro-2-methoxyphenyl)-7,8-dihydro-6*H*-cyclohepta[1,2-*d*:3,4-*d*′]bithiazole-2,2′-diamine 28.** An absolute ethanol (50 mL) suspension of **27** (1.73 g, 6.64 mmol) and **4** (2.11 g, 7.3 mmol) was heated at reflux overnight. EtOH was removed under reduced pressure and the residue was recrystallized from EtOH to yield **28** (2.1 g, 84%). ^{1}H NMR (400 MHz, DMSO-d_6): δ 9.81 (s, 1H), 9.19 (s, 2H), 8.44 (d, J = 2.4 Hz, 1H), 7.00 (d, J = 8.4 Hz, 1H), 6.92 (dd, J = 8.4 Hz, 2.4 Hz, 1H), 3.83 (s, 3H), 2.91−2.87 (m, 4H), 1.98 (m, 2H). ^{13}C NMR (100 MHz, DMSO-d_6): δ 167.6, 160.8, 147.0, 135.5, 131.7, 124.9, 122.0, 121.3, 117.2, 114.5, 112.6, 56.7, 28.9, 25.9, 21.9, 19.2. MS (ESI) *m*/*z* 378.88 $[M + 1]^+$.

***N*-(2-(5-Chloro-2-methoxyphenylamino)-7,8-dihydro-6*H*-cyclohepta[1,2-*d*:3,4-*d*′]bithiazole-2′-yl)pivalamide 29.** Compound **28** (1.73 g, 3.75 mmol) and dry DCM (40 mL) under N_2 was treated sequentially with TEA (1.32 mL, 9.38 mmol) and 2,2-dimethylpropionyl chloride (598 μL, 4.86 mmol). The suspension became light-brown within 2 min and DCM was removed in vacuo at room temperature. The residue was purified by flash chromatographic column (hexane/ethyl acetate = 4:1 and then 1:1 eluent) to afford **29** (1.46 g. 84%) with 99.0% purity. Mp decomposition at 197 °C. ^{1}H NMR (400 MHz, DMSO-d_6): δ 11.60 (s, 1H), 9.65 (s, 1H), 8.58 (d, J = 0.8 Hz, 1H), 6.99−6.92 (m, 2H), 3.84 (s, 3H), 3.01 (t, J = 4 Hz, 2H), 1.91 (t, J = 4 Hz, 2H), 1.99 (m, 2H), 1.21 (s, 9H). ^{13}C NMR (100 MHz, DMSO-d_6): δ 176.9, 160.1, 156.2, 146.9, 146.8, 138.1, 132.0, 125.0, 121.8, 120.9, 120.7, 117.2, 112.4, 56.7, 33.0, 27.3, 26.8, 23.0. HRMS *m*/*z* (ESI) calcd for $C_{21}H_{23}ClN_4O_2S_2$ $(M + H)^+$ 463.1024, found 463.1019.

2-(5-Chloro-2-methoxyphenylamino)-4,5,6,7-tetrahydrocyclohepta[*d*]thiazol-8-one 30. Following the procedure described for **26** by condensing 5-chloro-2-methoxyphenylthiourea gave **30** (light-brown solid; 26% for two steps). ^{1}H NMR (600 MHz, DMSO-d_6): δ 7.81 (d, J = 2.4 Hz, 1H), 7.75 (dd, J = 9 Hz, 2.4 Hz, 1H), 7.42 (d, J = 9 Hz, 1H), 3.83 (s, 3H), 2.84−2.75 (m, 2H), 2.58−2.52 (m, 1H), 2.33−2.28 (m, 1H), 1.90−1.74 (m, 4H). ^{13}C NMR (150 MHz, DMSO-d_6): δ 194.4, 169.8, 154.5, 148.9, 134.1, 130.2, 125.7, 122.6, 121.7, 116.3, 57.6, 42.9, 30.5, 24.4, 21.5.

7-Bromo-2-(5-chloro-2-methoxyphenylamino)-4,5,6,7-tetrahydrocyclohepta[*d*]thiazol-8-one 31. Following the procedure described for **27** gave **31** (white powder; 70% yield). MS (ESI) *m*/*z* $[M + H]^+$ 400.87; $[(M + 2) + H]^+$ 402.90.

***N*^{2}-(5-Chloro-2-methoxyphenyl)-5,6-dihydro-4*H*-cyclohepta[1,2-*d*:3,4-*d*′]bithiazole-2,2′-diamine 32.** Following the procedure outlined for **28** by condensing with thiourea afforded **32** as a white powder (32%). ^{1}H NMR (600 MHz, DMSO-d_6): δ 9.48 (br s, 1H), 7.89−7.84 (m, 2H), 7.81 (d, J = 2.4 Hz, 1H), 7.72 (dd, J = 9 Hz, 2.4 Hz, 1H), 7.40 (d, J = 9 Hz, 1H), 3.84 (s, 3H), 2.81−2.73 (m, 2H), 2.47−2.42 (m, 1H), 2.28−2.23 (m, 1H), 1.93−1.88 (m, 2H). ^{13}C NMR (150 MHz, DMSO-d_6): δ 166.7, 165.9, 154.0, 134.4, 134.0, 133.0, 129.6, 124.9, 121.7, 119.4, 115.4, 113.8, 56.8, 28.2, 25.3, 21.6. MS (ESI) *m*/*z* 379.01 $[M + 1]^+$.

***N*-(2-(5-Chloro-2-methoxyphenylamino)-5,6-dihydro-4*H*-cyclohepta[1,2-*d*:3,4-*d*′]bithi-azole-2′-yl)pivalamide 33.** Following the procedure outlined for **29** gave **33** as a yellow powder (36%). ^{1}H NMR (600 MHz, DMSO-d_6): δ 7.64 (d, J = 2.4 Hz, 1H), 7.62 (dd, J = 7.2 Hz, 2.4 Hz, 1H), 7.35 (d, J = 7.2 Hz, 1H), 7.05 (br s, 2H), 3.82 (s, 3H), 2.87−2.85 (m, 2H), 2.68−2.64 (m, 1H), 2.48−2.44 (m, 1H), 2.02−1.96 (m, 2H), 1.02 (s, 9H). ^{13}C NMR (150 MHz, DMSO-d_6): δ 187.3, 167.0, 165.8, 154.3, 137.4, 133.1, 131.1, 130.3, 127.3, 124.4, 118.5, 115.4, 114.7, 57.0, 40.7, 29.0, 28.3, 26.5, 22.8. HRMS *m*/*z* (ESI) calcd for $C_{21}H_{23}ClN_4O_2S_2$ $(M + H)^+$ 463.1024, found 463.1039.

Computational Methods. Model systems of **1**, **17**, **22**, and **29** with the *tert*-butyl group replaced by a methyl group and the methoxy and chloro groups on the aniline replaced by hydrogens were utilized. Preliminary calculations (see Figure S3 in Supporting Information) suggested that the presence of the methoxy and chloro functional groups does not significantly affect the relative energies of the two aniline conformers. In all cases, the lowest energy aniline and amide conformers (which are also consistent with the crystal structure of **29**; see Chart 2) were utilized.

All calculations were performed with the Gaussian 03[27] software suite. Geometries were optimized without symmetry constraints using the B3LYP/6-31+G(d,p) method.[28] All stationary points were characterized as either minima or transition state structures via frequency calculations, and the reported energies include unscaled

zero-point energy (ZPE) corrections. Single point calculations in water were completed utilizing the CPCM solvation model and UAKS radii.[29] Structural diagrams were produced using Ball & Stick, version 4.0.[30] See Supporting Information for coordinates of all computed structures and details on additional model systems.

Acknowledgment. The authors thank the Tara K. Telford Fund for Cystic Fibrosis Research at University of California—Davis, the National Institutes of Health (Grants DK072517 and GM076151), and the National Science Foundation [Grants CHE-0614756, CHE-0443516, CHE-0449845, CHE-9808183 (NMR spectrometers), and CHE-030089 (computer time from the Pittsburgh Supercomputer Center)] for their generous support. We thank Dr. Michael Bartberger (Amgen) for helpful insights.

Supporting Information Available: Figures S1−S5; spectral data of compounds **5**−**13**, **15**−**17**, **20**−**30**, **32**, and **33**; computational data; and X-ray crystallographic data for **29**. This material is available free of charge via the Internet at http://pubs.acs.org.

References

(1) Bobadilla, J. L.; Macek, M; Fine, J. P.; Farrell, P. M. Cystic fibrosis: a worldwide analysis of CFTR mutations. Correlation with incidence data and application to screening. *Hum. Mutat.* **2002**, *19*, 575–606.

(2) Pilewski, J. M.; Frizzell, R. A. Role of CFTR in airway disease. *Physiol. Rev.* **1999**, *79*, S215−S255.

(3) Sheppard, D. N.; Welsh, M. J. Structure and function of the CFTR chloride channel. *Physiol. Rev.* **1999**, *79*, S23−S45.

(4) (a) Denning, G. M.; Anderson, M. P.; Amara, J. F.; Marshall, J.; Smith, A. E.; Welsh, M. J. Processing of mutant cystic fibrosis transmembrane conductance regulator is temperature-sensitive. *Nature* **1992**, *358*, 761–764. (b) Lukacs, G. L.; Mohamed, A.; Kartner, N.; Chang, X.-B.; Riordan, J. R.; Grinstein, S. Conformational maturation of CFTR but not its mutant counterpart (ΔF508) occurs in the endoplasmic reticulum and requires ATP. *EMBO J.* **1994**, *13*, 6076–6086. (c) Kopito, R. R. Biosynthesis and degradation of CFTR. *Physiol. Rev.* **1999**, *79*, S167−S173. (d) Du, K.; Sharma, M.; Lukacs, G. L. The ΔF508 cystic fibrosis mutation impairs domain−domain interactions and arrests post-translational folding of CFTR. *Nat. Struct. Mol. Biol.* **2005**, *12*, 17–25.

(5) (a) Carlile, G. W.; Robert, R.; Zhang, D.; Teske, K. A.; Luo, Y.; Hanrahan, J. W.; Thomas, D. Y. Correctors of protein trafficking defects identified by a novel high-throughput screening assay. *ChemBioChem* **2007**, *8*, 1012–1020. (b) Becq, F. On the discovery and development of CFTR chloride channel activators. *Cur. Pharm. Des.* **2006**, *12*, 471–484. (c) Van Goor, F.; Straley, K. S.; Cao, D.; Gonzalez, J.; Hadida, S.; Hazlewood, A.; Joubran, J.; Knapp, T.; Makings, L. R; Miller, M.; Neuberger, T.; Olson, E.; Panchenko, V.; Rader, J.; Singh, A.; Stack, J. H.; Tung, R.; Grootenhuis, P. D. J.; Negulescu, P. Rescue of DeltaF508-CFTR trafficking and gating in human cystic fibrosis airway primary cultures by small molecules. *Am. J. Physiol.* **2006**, *290*, L1117–L1130.

(6) Yang, H.; Shelat, A. A.; Guy, R. K.; Gopinath, V. S.; Ma, T.; Du, K.; Lukacs, G. L.; Taddei, A.; Folli, C.; Pedemonte, N.; Galietta, L. J. V.; Verkman, A. S. Nanomolar affinity small molecule correctors of defective ΔF508-CFTR chloride channel gating. *J. Biol. Chem.* **2003**, *278*, 35079–35085.

(7) (a) Galietta, L. J.; Haggie, P. M.; Verkman, A. S. Green fluorescent protein-based halide indicators with improved chloride and iodide affinities. *FEBS Lett.* **2001**, *499*, 220–224. (b) Pedemonte, N.; Lukacs, G. L.; Du, K.; Caci, E.; Zegarra-Moran, O.; Galietta, L. J. V.; Verkman, A. S. Small-molecule correctors of defective ΔF508-CFTR cellular processing identified by high-throughput screening. *J. Clin. Invest.* **2005**, *115*, 2564–2571.

(8) (a) Illek, B.; Fischer, H.; Santos, G. F.; Widdicombe, J. H.; Machen, T. E.; Reenstra, W. W. cAMP-independent activation of CFTR Cl channels by the tyrosine kinase inhibitor genistein. *Am. J. Physiol.* **1995**, *268*, C886−C893. (b) Schmidt, A.; Hughes, L. K.; Cai, Z.; Mendes, F.; Li, H.; Sheppard, D. N.; Amaral, M. D. Prolonged treatment of cells with genistein modulates the expression and function of the cystic fibrosis transmembrane conductance regulator. *Br. J. Pharmacol.* **2008**, *153*, 1311–1323.

(9) Hwang, T.-C.; Horie, M.; Nairn, A. C.; Gadsby, D. C. Role of GTP-binding proteins in the regulation of cardiac chloride conductance. *J. Gen. Physiol.* **1992**, *99*, 465–489.

(10) Kikelj, D.; Urleb, U. Product class 17: thiazoles. *Sci. Synth.* **2002**, *11*, 627–833.

(11) Yoo, C. L.; Yu, G. J.; Yang, B.; Robins, L. I.; Verkman, A. S.; Kurth, M. J. 4′-Methyl-4,5′-bithiazole-based correctors of defective ΔF508-CFTR cellular processing. *Bioorg. Med. Chem. Lett.* **2008**, *18*, 2610–2614.

(12) (a) Ahmed, Z.; Langer, P. Synthesis of functionalized diaryl ethers by [3 + 3] cyclization of 1,3-bis(silyl enol ethers) with 2-aryloxy-3-(silyloxy)alk-2-en-1-ones. *Synlett* **2006**, 3361–3363. (b) Hayakawa, M.; Kaizawa, H.; Kawaguchi, K.-I.; Ishikawa, N.; Koizumi, T.; Ohishi, T.; Yamano, M.; Okada, M.; Ohta, M.; Tsukamoto, S.-I.; Raynaud, F. I.; Waterfield, M. D.; Parker, P.; Workman, P. Synthesis and biological evaluation of imidazo[1,2-*a*]pyridine derivatives as novel PI3 kinase p110a inhibitors. *Bioorg. Med. Chem.* **2007**, *15*, 403–412. (c) El-Gazzar, A. B. A.; Hussein, H. A. R.; Aly, A. S. Synthesis and reactions of polynuclear heterocycles: azolothienopyrimidines and thienothiazolopyrimidines. *Phosphorus, Sulfur Silicon Relat. Elem.* **2006**, *181*, 2771–2784. (d) McInnes, C.; Wang, S.; Anderson, S.; O'Boyle, J.; Jackson, W.; Kontopidis, G.; Meades, C.; Mezna, M.; Thomas, M.; Wood, G.; Lane, D. P.; Fischer, P. M. Structural determinants of CDK4 inhibition and design of selective ATP competitive inhibitors. *Chem. Biol.* **2004**, *11*, 525–534.

(13) Prepared by analogy with methodology reported in the following: Boyer, C.; Finazzi, G.; Laurent, P.; Haas, A.; Blancou, H. Synthesis and photosynthetic inhibition activity of substituted 5-[bis(trifluoromethyl)methyl]-2-aminothiazoles. *J. Fluorine Chem.* **2006**, *127*, 1522–1527.

(14) Sayed, S. M.; Raslan, M. A.; Khalil, M. A.; Dawood, K. M. Synthesis and reactivity of cyanomethyl 2-amino-4-methylthiazolyl ketone. A facile synthesis of novel pyrazolo[5,1-*c*]-1,2,4-triazine, 1,2,4-triazolo[5,1-*c*]-1,2,4-triazine, 1,2,4-triazino[4,3-*a*]benzimidazole, pyridazin-6-imine and 6-oxopyridazinone derivatives. *Heteroat. Chem.* **1999**, *10*, 385–390.

(15) Yoo, C. L.; Fettinger, J. C.; Kurth, M. J. Stannous chloride in alcohol: a one-pot conversion of 2-nitro-*N*-arylbenzamides to 2,3-dihydro-1*H*-quinazoline-4-ones. *J. Org. Chem.* **2005**, *70*, 6941–6943.

(16) See, for example, the following: (a) Angyan, J.; Poirier, R. A.; Kucsman, A.; Csizmadia, I. G. Bonding between nonbonded sulfur and oxygen atoms in selected organic molecules (a quantum chemical study). *J. Am. Chem. Soc.* **1987**, *109*, 2237–2245. (b) Meyer, E.; Joussef, A. C.; Gallardo, H.; Bortoluzzi, A. J.; Longo, R. L. 1,5-Type nonbonded O···S and S···S interactions in (acylimino) and (thioacylimino)benzothiazoline systems. Crystal structures and theoretical calculations. *Tetrahedron* **2003**, *59*, 10187–10193. (c) Iwaoka, M.; Takemoto, S.; Okada, M.; Tomoda, S. Weak nonbonded S···X (X = O, N, and S) interactions in proteins. Statistical and theoretical studies. *Bull. Chem. Soc. Jpn.* **2002**, *75*, 1611–1625. (d) Pomerantz, M. Planar 2,2′-bithiophenes with 3,3′- and 3,3′-,4,4′-substituents. A computational study. *Tetrahedron Lett.* **2003**, *44*, 1563–1565. (e) Rábai, J.; Kapovits, I.; Jalsovszky, I.; Argay, Gy.; Fülöp, V.; Kálmán, A.; Koritsánszky, T. Molecular structures of cyclic sulfilimines without and with intramolecular sulfur−oxygen interaction: an X-ray study. *J. Mol. Struct.* **1996**, *382*, 13–21. (f) Kucsman, Á.; Kapovits, I.; Párkányi, L.; Kálmán, A. Conformation of diaryl sulphides with intramolecular sulphur(II)−oxygen interaction: an X-ray study of methyl 2-(4-nitrophenylthio)benzoate and 2-diazoacetyl-4′-nitrodiphenyl sulphide. *J. Mol. Struct.* **1986**, *140*, 141–150.

(17) In **1**, the computed gas-phase penalty associated with a 180° rotation about the $C_{thiazole}-N_{amide}$ bond is approximately 9 kcal/mol. This likely reflects both the loss of the favorable S···O interaction and the addition of an unfavorable O···N interaction.

(18) One might expect that the twisted nature of the *s-trans* structure results from a $C(4')-CH_3$ steric interaction with a phenyl hydrogen (see Figure 2a). However, rotation of the phenylamine group to the alternative conformation (which can occur with a barrier of approximately 4−6 kcal/mol) results in a structure that is slightly higher in energy and slightly more twisted (see Computational Methods and Figures S3 and S4 in the Supporting Information).

(19) Lipinski, C. A.; Blizniak, T. E.; Craig, R. H. An improved preparation and use of 2-bromoacetoacetaldehyde in a new synthesis of 2-substituted-4-acetylimidazoles. *J. Org. Chem.* **1984**, *49*, 566–570.

(20) Matulenko, M. A.; Lee, C.-H.; Jiang, M.; Frey, R. R.; Cowart, M. D.; Bayburt, E. K.; DiDomenico, S.; Gfesser, G. A.; Gomtsyan, A.; Zheng, G. Z.; McKie, J. A.; Stewart, A. O.; Yu, H.; Kohlhaas, K. L.; Alexander, K. M.; McGaraughty, S.; Wismer, C. T.; Mikusa, J.; Marsh, K. C.; Snyder, R. D.; Diehl, M. S.; Kowaluk, E. A.; Jarvis, M. F.; Bhagwat, S. S. 5-(3-Bromophenyl)-7-(6-morpholin-4-ylpyridin-3-yl)pyrido[2,3-*d*]pyrimidin-4-ylamine: structure−activity relationships of 7-substituted heteroaryl analogs as non-nucleoside adenosine kinase inhibitors. *Bioorg. Med. Chem.* **2005**, *13*, 3705−3720.

(21) Kochetkov, N. K.; Nifant'ev, E. E.; Molodtsov, N. V. Bromination of -oxo acetals. *Zh. Obshch. Khim.* **1959**, *29*, 23302337.

(22) (a) Katritzky, A. R.; Laurenzo, K. S.; Relyea, D. I. The preparation and fungicidal activity of a series of thiazolyl- and isothiazolyldiarylcarbinols. *Can. J. Chem.* **1988**, *66*, 1617–1624. (b) Chen, Y. L.; Cherry, K.; Corman, M. L.; Ebbinghaus, C. F.; Gamlath, C. B.; Liston, D.; Martin, B.-A.; Oborski, C. E.; Sahagan, B. G. Thiazole−diamides as

potent γ-secretase inhibitors. *Bioorg. Med. Chem. Lett.* **2007**, *17*, 5518–5522.

(23) Van der Mey, M.; Bommele, K. M.; Boss, H.; Hatzelmann, A.; Van Slingerland, M.; Sterk, G. J.; Timmerman, H. Synthesis and structure−activity relationships of *cis*-tetrahydrophthalazinone/pyridazinone hybrids: a novel series of potent dual PDE3/PDE4 inhibitory agents. *J. Med. Chem.* **2003**, *46*, 2008–2016.

(24) Kreutzberger, A.; Schimmelpfennig, H. Antiviral drugs. XVIII. 2-Aminothizaoles by cleavage of the S−S bond of disulfidodicarbamidine. *Arch. Pharm. (Weinheim, Ger.)* **1981**, *314*, 385–391.

(25) Schiavi, B.; Ahond, A.; Al-Mourabit, A.; Pupat, C.; Chiaroni, A.; Gaspard, C.; Potier, P. Synthesis of 5-deazathiogirolines: analogs of a natural antitumor agent. *Tetrahedron* **2002**, *58*, 4201–4215.

(26) (a) Ragan, J. A.; Makowski, T. W.; Am Ende, D. J.; Clifford, P. J.; Young, G. R.; Conrad, A. K.; Eisenbeis, S. A. A practical synthesis of 1,3-cycloheptanedione. *Org. Process Res. Dev.* **1998**, *2*, 379–381. (b) Bhushan, V.; Chandrasekaran, S. A convenient synthesis of cycloheptane-1,3-dione. *Synth. Commun.* **1984**, *14*, 339–345.

(27) Frisch, M. J.; et al. *Gaussian 03*, revision D.01; Gaussian, Inc.: Pittsburgh, PA, 2003 (full reference in Supporting Information).

(28) (a) Becke, A. D. Density-functional thermochemistry. III. The role of exact exchange. *J. Chem. Phys.* **1993**, *98*, 5648–5652. (b) Becke, A. D. A new mixing of Hartree−Fock and local-density-functional theories. *J. Chem. Phys.* **1993**, *98*, 1372–1377. (c) Lee, C.; Yang, W.; Parr, R. G. Development of the Colle−Salvetti correlation-energy formula into a functional of the electron density. *Phys. Rev. B* **1988**, *37*, 785–789. (d) Stephens, P. J.; Devlin, F. J.; Chabalowski, C. F.; Frisch, M. J. Ab initio calculation of vibrational absorption and circular dichroism spectra using density functional force fields. *J. Phys. Chem.* **1994**, *98*, 11623–11627.

(29) (a) Barone, V.; Cossi, M. J. Quantum calculation of molecular energy gradients in solution by a conductor solvent model. *J. Phys. Chem. A* **1998**, *102*, 1995–2001. (b) Barone, B.; Cossi, M.; Tomasi, J. Geometry optimization of molecular structures in solution by the polarizable continuum model. *J. Comput. Chem.* **1998**, *19*, 404–417. (c) Takano, Y.; Houk, K. N. Benchmarking the conductor-like polarizable continuum model (CPCM) for aqueous solvation free energies of neutral and ionic organic molecules. *J. Chem. Theor. Comput.* **2005**, *1*, 70–77.

(30) Müller, N.; Falk, A.; Gsaller, G. *Ball & Stick, Molecular Graphics Application for MacOS Computers*, version 4.0a12; Johannes Kepler University: Linz, Austria, 2004.

JM800533C